Philosophical Magazine A

ISSN: 0141-8610 (Print) 1460-6992 (Online) Journal homepage: https://www.tandfonline.com/loi/tpha20

A high-resolution electron microscopy study of secondary dislocations in Σ = 3, [ī10]—(ī1) grain boundaries of aluminium

M. Shamzuzzoha , P. A. Deymier & D. J. Smith

To cite this article: M. Shamzuzzoha , P. A. Deymier & D. J. Smith (1991) A high-resolution electron microscopy study of secondary dislocations in Σ = 3, [ī10]—(ī1) grain boundaries of aluminium, Philosophical Magazine A, 64:1, 245-253, DOI: 10.1080/01418619108206138

To link to this article: https://doi.org/10.1080/01418619108206138

PHILOSOPHICAL MAGAZINE A, 1991, VOL. 64, NO. 1, 245–253

A high-resolution electron microscopy study of secondary dislocations in $\Sigma = 3, [\bar{1}10]$–$(\bar{1}\bar{1}1)$ grain boundaries of aluminium

By M. SHAMZUZZOHA and P. A. DEYMIER

Department of Materials Science and Engineering,
University of Arizona, Tucson, Arizona 85721, USA

and DAVID J. SMITH

Center for Solid State Science and Department of Physics,
Arizona State University, Tempe, Arizona 85287, USA

[*Received 4 September 1989*† *and accepted 26 June 1990*]

ABSTRACT

The atomic structure of secondary dislocations at $\Sigma = 3, [\bar{1}10]$–$(\bar{1}\bar{1}1)$ grain boundaries in pure aluminium have been studied by high-resolution electron microscopy. In defect-free regions, the grain boundary coincident-site lattice is continuous across the interface but several different secondary grain-boundary dislocations are observed in the vicinity of interplanar steps.

§ 1. INTRODUCTION

The structures of grain boundaries and associated defects have been the subject of many investigations ever since it was realized that they exerted a critical influence in controlling the properties of polycrystalline materials. Various grain-boundary models have been proposed to explain the relationships between grain-boundary structures and their properties.

The concepts of coincident-site lattice (CSL) (Kronberg and Wilson 1964), displacement shift complete (DSC) lattice (Bollmann 1970, Balluffi 1977, Smith and Pond 1976) and the O-lattice model (Bollmann 1970), developed on the basis of various proposals put forward by Kronberg and Wilson (1964) and Frank (1955), and elaborated by Brandon, Ralph, Raganathan and Wald (1964), have been gaining popularity in describing grain-boundary structure. The remarkable aspect regarding these models is contained in the ordered structure along the boundary, where two adjoining interface lattices of identical cell dimensions form a dichromatic pattern of three-dimensional periodicity. The CSL describes the periodicity of this dichromatic pattern but can only characterize dislocation-free grain boundaries. The DSC lattice is a reciprocal lattice of the CSL and defines all vector displacements between the two interpenetrating lattices which conserve the dichromatic pattern by a pattern shift. The DSC lattice can therefore characterize interfacial line defects near coincidence large-angle grain boundaries.

† Received in final form 22 June 1990.

Any grain-boundary structure is fundamentally determined by the manner in which atoms of the boundary relax to minimize energy. From the principle of CSL and DSC lattice theory framework, lattice translations in such relaxed structures may be accounted for in terms of a DSC lattice dislocation network. The main limitation of these dislocation theories lies in the fact that they are based on the assumption of rigid lattices and they take no consideration of possible distortions that exist in the relaxed structure of grain boundaries.

There is strong experimental evidence to support the CSL and DSC lattice dislocation models. Transmission electron microscopy methods involving analyses of grain-boundary fringe contrast (Pond 1979) applied to various large-angle grain boundaries of cubic crystals (Balluffi, Koman and Schober 1972, Pond, Smith and Clark 1974, Forwood and Clarebrough 1977, Balluffi, Bristowe and Sun 1981, Vaudin, Cunningham and Ast 1983) confirmed that arrays of dislocations with DSC Burgers vectors accommodated deviations from specific misorientations, although they revealed very little about the actual relaxed core structures of the grain boundaries. Relaxation associated with such grain boundaries usually extends over a distance of a few atomic diameters and thus cannot be revealed by fringe contrast electron microscopy. The only experimental technique which can be applied to obtain this information directly is the observation of atomic images using high-resolution electron microscopy (HREM).

Recent observations of a $\Sigma=3,(112)$ twin boundary in germanium by HREM (Bourret and Bacmann 1985) has already revealed major characteristics of grain-boundary defects and dislocations. The present communication deals with a similar HREM study which is aimed at elucidating the relaxed structure of various defects present in a $\Sigma=3,[\bar{1}10]$–$(\bar{1}\bar{1}1)$ twin boundary in aluminium.

§2. Experimental details

Plate-shaped single crystals of aluminium with a nominal purity of 99·999% were cross-rolled to 92% reduction with a low reduction rate per pass and then annealed at 300°C for 1 h. The annealed crystals were longitudinally strained to 0·5% reduction and then re-annealed at 600°C for another hour. Upon metallographic examination, the re-annealed crystals typically revealed the presence of several twins.

For thin-foil preparation, cylindrical specimens of 3 mm diameter containing these twin boundaries were trepanned from the grown samples with a spark-cutting machine. The cylinders were then sliced with a diamond saw to a thickness of 0·5 mm and then ground gently on 600 grade silicon carbide paper to about 200 μm. Finally, the discs were electropolished at a voltage of 10 V at room temperature in a solution of 100 cm^3 of perchloric acid and 900 cm^3 of methanol diluted to 80% by glycerol. Polishing was halted just after perforation.

The thin foils thus prepared were examined with a 200 kV Hitachi electron microscope, and angle and axis orientations of the twin boundaries were determined. HREM was performed with a JEM 4000EX operated at 400 kV. In both electron microscopes, the specimen was usually tilted to align the direction of the electron beam with a $\langle 110\rangle$ projection of the aluminium bicrystal. The high-resolution electron micrographs shown here were typically recorded as part of a through-focal series at a magnification of 500 000 ×. Images recorded near the Scherzer defocus should permit intuitive interpretation in terms of atom column positions to within about 0·3 Å (Saxton and Smith 1985).

§3. Results

A HREM image with simultaneous lattice imaging conditions in adjacent grains of a $\Sigma=3, [\bar{1}10]$–$(\bar{1}\bar{1}1)$ twin boundary for aluminium is shown in fig. 1. Most of the defect image exhibits a perfect twin-boundary structure in which all atomic sites across the interface are coincident with $(\bar{1}\bar{1}1)$ planes of an angle of 70·52°. However, this twin boundary also displayed a variety of irregularities; one such irregularity is present at the position marked A in fig. 1.

Irregularity at a grain boundary must always be associated with defects present in the boundary. A discussion of the defects present in a $\Sigma=3$ boundary structure requires a comparison with the theoretically predicted boundary structure. The geometrical analysis of a $\Sigma=3$ twin boundary for cubic crystals by Bollmann (1970) suggests that the Burgers vectors for secondary grain-boundary dislocations (SGBDs), associated with grain-boundary defects, should belong to the $\Sigma=3$ DSC lattice vectors. These vectors **b**, measuring the displacement of equivalent sets of grain-boundary planes, could be either $\mathbf{b}_1=\frac{1}{6}[112]$ and $\mathbf{b}_2=\frac{1}{6}[2\bar{1}1]$ (which lie on two $\langle 110\rangle$ normals to the twin-boundary plane) or $\mathbf{b}_3=\frac{1}{3}\langle 111\rangle$ (which lies along the twin-boundary normal). The particular operating vector can be directly obtained from the HREM micrograph, using a Frank dislocation circuit applied to the corresponding defects present in the boundary. According to Hirth and Balluffi (1973), the CSL across this grain boundary, containing defects with a $\Sigma=3$ DSC lattice Burgers vector, can only be continuous if the boundary plane undergoes a translation of one monolayer interatomic spacing along the boundary normal. In a $\Sigma=3$ grain boundary a step is thus always associated with a dislocation corresponding to a DSC lattice Burgers vector. Three successive steps, each with a dislocation Burgers vector of the type $\frac{1}{3}\langle 111\rangle$, then correspond to a dislocation with a lattice Burgers vector.

3.1. *SGBDs in $\Sigma=3, [\bar{1}10]$–$(\bar{1}\bar{1}1)$ boundary with a DSC lattice Burgers vector*

The atomic arrangements around a defect on an otherwise step-free $\Sigma=3, [\bar{1}10]$–$(\bar{1}\bar{1}1)$ twin boundary can be deduced from the micrograph shown in fig. 2(*a*), as drawn in fig. 2(*b*). A Frank dislocation circuit applied to the defect indicates an in-plane closure failure of $\frac{1}{6}[112]$, which corresponds to a $\Sigma=3$ DSC lattice Burgers vector

Fig. 1

High-resolution electron micrograph of a $\Sigma=3$ grain boundary in aluminium, with the incident beam direction parallel to the $(\bar{1}11)$ twinning plane and normal to the $(\bar{1}10)$ plane. Atomic column positions are represented by black spots.

Fig. 2

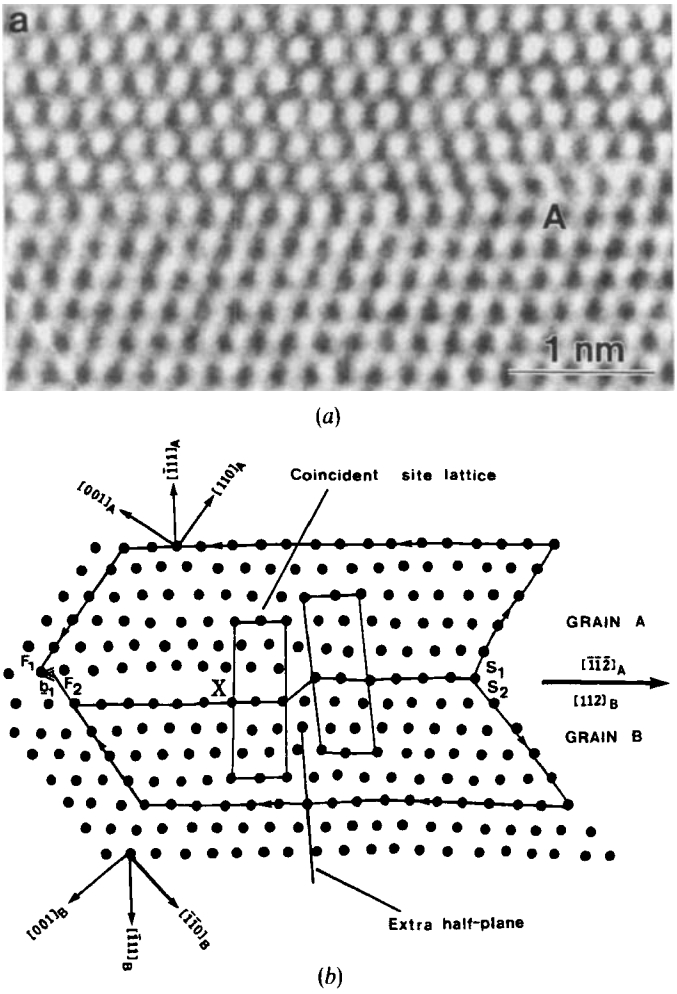

(*a*) HREM image of a SGBD with a $\mathbf{b}_1$ Burgers vector and step corresponding to one $[\bar{1}\bar{1}1]$ interplanar spacing. (*b*) Orientation relationships model of a $\mathbf{b}_1$ SGBD projected on the $(\bar{1}10)$ plane of the $\mathbf{b}_1$ SGBD, as drawn from the HREM image. A delocalization of the dislocation core across the twinning plane is apparent at the position marked A.

($\mathbf{b}_1$) for the dislocation associated with the defect. The CSL across the twin boundary is continuous at step-free regions but translates by a vector $\mathbf{t} \approx \frac{1}{2}[00\bar{1}]$ at the extra atomic half-plane corresponding to the dislocation. This results in a grain-boundary step of one monolayer atomic spacing along the grain-boundary normal, that is along $[\bar{1}\bar{1}1]$.

As it approaches the interplanar step, the grain boundary appears to adopt an atomic structure which is not typical of a localized dislocation core. Structural comparison with the HREM image of a neighbouring defect-free portion of the $\Sigma = 3, [\bar{1}10]$–$(\bar{1}\bar{1}1)$ twin boundary obtained under identical experimental conditions indicates that the dislocation cores is replaced by a progressive translational mismatch amounting to a vector $\mathbf{t} = \frac{1}{6}[112]$ of CSL planes across the boundary. The interface

Fig. 3

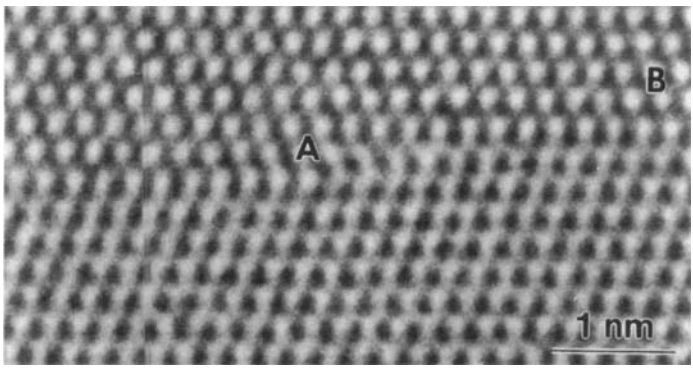

High-resolution image of a $\Sigma = 3$ grain boundary projected onto the $(\bar{1}10)$ plane showing two grain-boundary steps, labelled A and B, separated by a region containing a relaxed dislocation core. Each dislocation associated with a boundary step has a $\mathbf{b}_1$ Burgers vector.

gradually changes from a completely coherent coincident boundary to a slightly non-coherent grain boundary in the vicinity of the dislocation core. This results in a delocalization of the SGBDs along the interface extending over a distance of approximately 0·9 nm along the grain-boundary axis.

Since a step associated with a dislocation of Burgers vector $\mathbf{b}_1$ requires a prior delocalization of SGBDs in the grain boundary, it appears unlikely that two or more successive grain-boundary steps (associated with a $\mathbf{b}_1$ dislocation Burgers vector) with no delocalization of the SGBDs can be present in the boundary. In the present study no such incident occurs. However, such steps were observed repeatedly but separated by the substantial boundary length which is required to accommodate delocalization. Figure 3 shows an example of multiple grain-boundary stepping.

Another defect at a $\Sigma = 3, [\bar{1}10]$–$(\bar{1}\bar{1}1)$ twin boundary in aluminium is shown in fig. 4. The Burgers vector determined by the use of a Frank dislocation circuit (fig. 4 (*b*)) on the defect present at the grain boundary is $\frac{1}{3}[\bar{1}\bar{1}1]$ which is again a $\Sigma = 3$, DSC lattice vector ($\mathbf{b}_3$) perpendicular to the grain-boundary plane. The CSL across this boundary is also continuous at step-free regions but, contrary to the theoretical dislocation model, its continuity at the onset of the extra half-plane remains conserved by a vector translation of $\frac{1}{2}[110]$. This allows the CSL to shift one stacking layer along $[\bar{1}10]$ and enables the grain boundary to undergo a monolayer atomic stepping along the grain-boundary normal, that is along $[\bar{1}\bar{1}1]$.

Comparison of the interphase CSL lattice points bordering the boundary with their counterparts in a neighbouring defect-free $\Sigma = 3, [\bar{1}10]$–$(\bar{1}\bar{1}1)$ twin boundary imaged under identical experimental conditions reveals that the dislocation is localized. The coherency of the twin plane is maintained by a relative translation $\mathbf{t} = \frac{1}{6}[112]$ of the (001) planes across the twin boundary. This translation takes place on the side of the bicrystal which does not contain the extra $(\bar{1}\bar{1}1)$ half-plane. A lack of such prior delocalization of atomic arrangements in the wake of such a boundary step (with $\mathbf{b}_3$ dislocation Burgers vector) suggests that multiple steps exhibiting a rather small interstep boundary should be present in relaxed $\Sigma = 3$ grain boundaries. One such example is shown in fig. 5.

Fig. 4

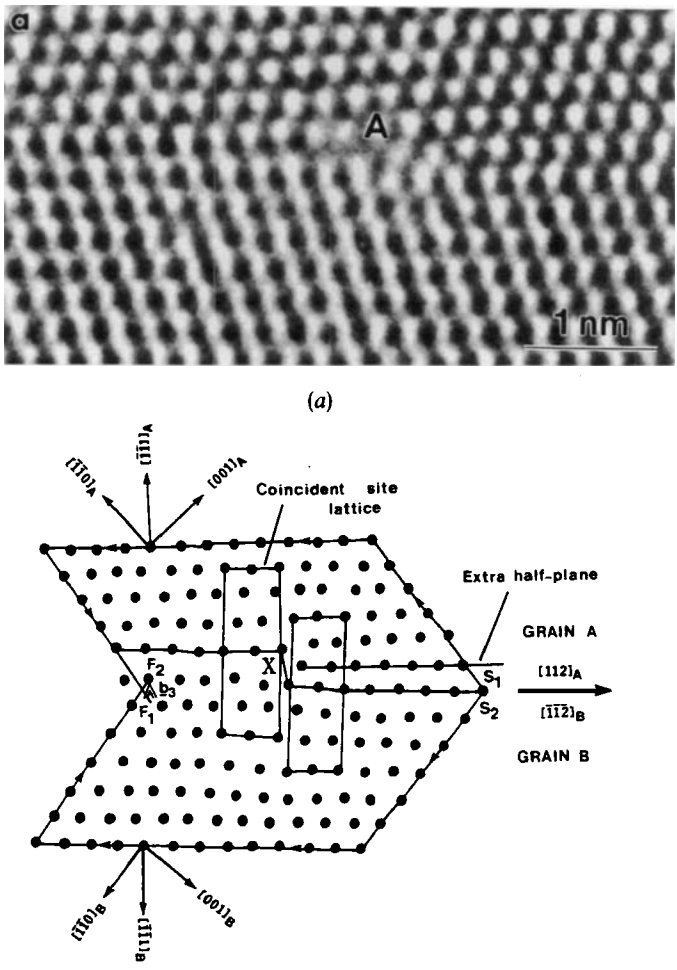

(*a*)

(*b*)

(*a*) HREM image of a SGBD with a $\mathbf{b}_3$ Burgers vector and slip corresponding to one $[\bar{1}\bar{1}1]$ interplanar spacing. (*b*) Orientation relationships of twin with a $\mathbf{b}_3$ SGBD projected on the $(\bar{1}10)$ plane as drawn from the HREM image. Some relaxation of the dislocation core across the twinning plane is apparent at the position marked A.

The grain boundary in fig. 6 seems to be unique in the sense that the defect present does not appear to produce any visible grain-boundary step. A Frank dislocation circuit, when applied to the defect, gives an apparent Burgers vector of magnitude $|\mathbf{b}_1| \cos 60°$, which lies on the twin plane. Among the possible $\Sigma = 3$ DSC lattice vectors, only $\frac{1}{6}[2\bar{1}1]$ projects onto $(\bar{1}10)$ with such a magnitude, indicating that the true Burgers vector of this grain-boundary defect is the DSC lattice vector $\mathbf{b}_2$. A schematic representation of the geometry of this defect in a $\Sigma = 3$ twin boundary is given in fig. 6(*b*). The Burgers vector $\mathbf{b}_2$ lies on the twin-boundary plane $(\bar{1}\bar{1}1)$ and makes an angle of 30° with $[\bar{1}10]$. In association with the defect, the grain boundary undergoes monolayer atomic stepping along the $[\bar{1}\bar{1}1]$ grain-boundary normal with the stepping

Fig. 5

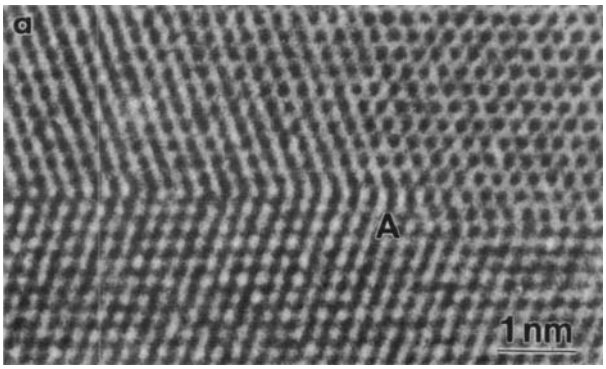

(*a*)

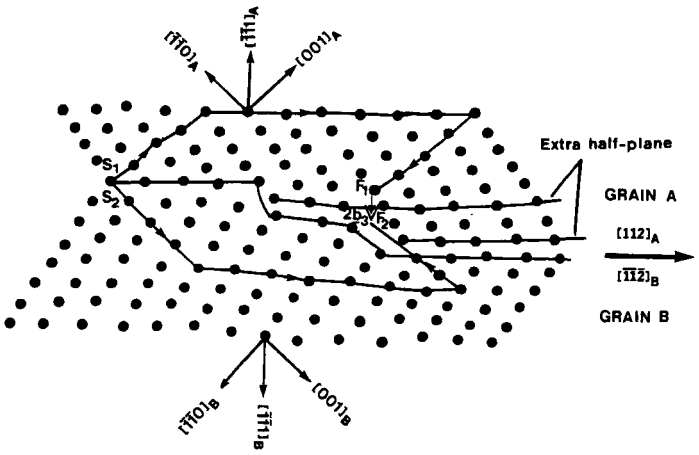

(*b*)

(*a*) HREM image of a $\Sigma = 3$ grain boundary projected on the $(\bar{1}10)$ plane showing a double interplanar stepping, marked A, at the twinning plane. (*b*) Orientation relationships in the twinned atomic configuration of (*a*) projected onto one stacking layer of the $(\bar{1}10)$ plane.

plane also normal to $\mathbf{b}_2$. Under such conditions, the plane of the step will not be $(\bar{1}10)$ and it will therefore not be visible in a $[\bar{1}10]$ cross-section image of this twin boundary.

Similar to the $\mathbf{b}_1$ or $\mathbf{b}_3$ SGBD, either a delocalization or a localization of the $\mathbf{b}_2$ SGBD should be present in the twin boundary. Either of these SGBD interactions should result in a translational shift (parallel to $\mathbf{b}_2$) of atoms on the side of the twin plane containing the defect. The overall effect of this displacement of atoms is the development of some non-uniform atomic columns along $[\bar{1}10]$ in the specific grain. The HREM image taken in the $[\bar{1}10]$ projection of such a grain boundary (fig. 6(*a*)) confirms this situation since one side of the twin is imaged as a region of poor contrast.

Fig. 6

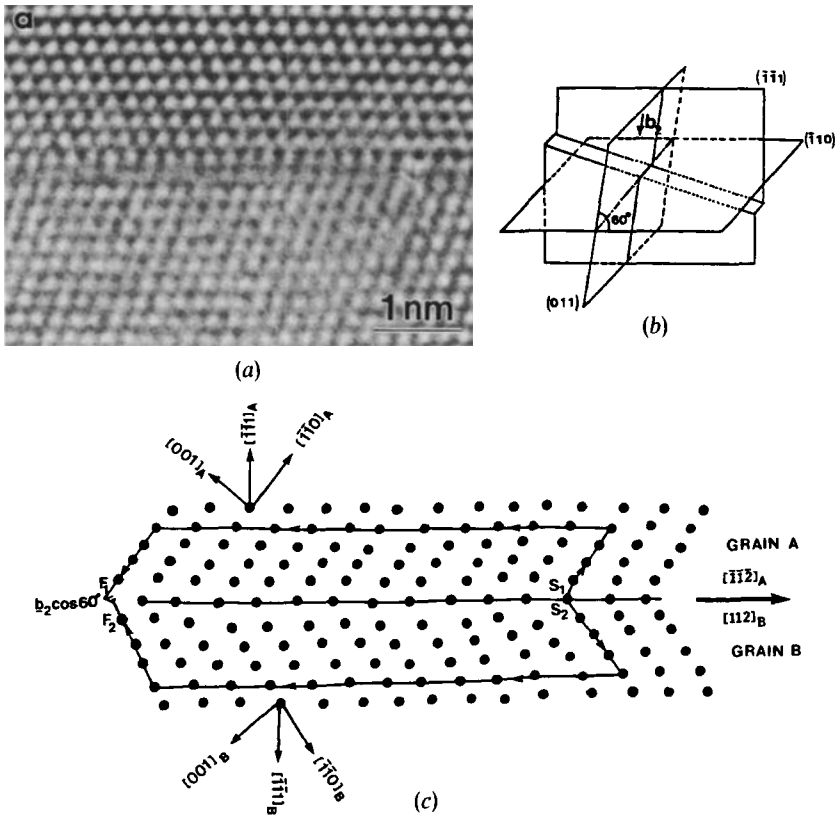

(*a*) HREM image of a $\Sigma = 3$ SGBD projected on the $(\bar{1}10)$ plane showing the trace of the step associated with the $\mathbf{b}_3$ SGBD. (*b*) Schematic diagram showing the spatial orientation of a $\mathbf{b}_3$ SGBD with respect to the twinning plane. (*c*) Orientation relationships in the twinned atomic configuration projected on the $(\bar{1}10)$ plane, as drawn from the HREM image.

§4. Conclusion

In light of this study, the following conclusions can be made.

(1) The Burgers vectors observed for SGBD in the relaxed $\Sigma = 3$, $[\bar{1}10]$–$(\bar{1}\bar{1}1)$ grain boundary of aluminium are completely in accord with theoretical predictions based on CSL and DSC lattice dislocation theories.

(2) There are some significant differences between the predicted core structure of SGBDs and the actual structure.

(3) SGBDs with Burgers vectors in the plane of the twin exhibit a delocalization, resulting in an alteration of the translational state of the twin. This delocalization gives rise to slight bending of a $(\bar{1}\bar{1}1)$ lattice plane in the vicinity of the interfacial step.

(4) An SGBD with a Burgers vector perpendicular to the grain-boundary plane shows very little relaxation. In the wake of the interfacial step associated with this SGBD, the continuation of the CSL is conserved by its translation, which required combined shifts of monatomic stepping along the grain-boundary normal and plane.

ACKNOWLEDGMENTS

This research was supported in part by the Facility for High Resolution Electron Microscopy in the Center for Solid State Science at Arizona State University, established with support from the National Science Foundation (Grant DMR-86-11609). The authors also acknowledge the receipt of financial support from the U.S. Department of Energy under Contract DE-FG02-87ER45285.

REFERENCES

BALLUFFI, R. W., 1977, *Interfacial Segregation* (Metals Park, Ohio: American Society for Metals).
BALLUFFI, R. W., BRISTOWE, P. D., and SUN, C. P., 1981, *J. Am. Ceram. Soc.*, **64**, 23.
BALLUFFI, R. W., KOMEN, Y., and SCHOBER, T., 1972, *Surf. Sci.*, **31**, 68.
BOLLMANN, W., 1970, *Crystal Defects and Crystalline Interfaces* (New York: Springer).
BOURRET, A., and BACMANN, J. J., 1985, Institute of Physics Conference Series No. 78 (Bristol: Institute of Physics), p. 337.
BRANDON, D. G., RALPH, B., RAGANATHAN, S., and WALD, M. S., 1964, *Acta metall.*, **12**, 813.
FORWOOD, C. T., and CLAREBROUGH, L. M., 1977, *Phil. Mag.*, **36**, 1131.
FRANK, F. C., 1955, *Conference on Defects in Crystalline Solids* (London: Physical Society).
HIRTH, J. P., and BALLUFFI, R. W., 1973, *Acta metall.*, **21**, 929.
KRONBERG, M. L., and WILSON, F. M., 1964, *Trans. AIME*, **85**, 26.
POND, R. C., 1979, *J. Microsc.*, **116**, 105.
POND, R. C., and BOLLMANN, W., 1979, *Phil. Trans. R. Soc.*, **292**, 449.
POND, R. C., SMITH, D. A., and CLARK, W. A. T., 1974, *J. Microsc.*, **102**, 309.
SAXTON, W. O., and SMITH, D. J., 1985, *Ultramicroscopy*, **18**, 39.
SMITH, D. A., and POND, R. C., 1976, *Int. Metals Rev.*, **205**, 61.
VAUDIN, M., CUNNINGHAM, B., and AST, D. G., 1983, *Scripta metall.*, **17**, 191.